



Article

Satellite-Based Estimation of Roughness Length over Vegetated Surfaces and Its Utilization in WRF Simulations

Yiming Liu ^{1,2,3} , Chong Shen ^{4,*}, Xiaoyang Chen ^{5,6}, Yingying Hong ⁷, Qi Fan ^{1,2,3}, Pakwai Chan ⁸ , Chunlin Wang ^{3,4} and Jing Lan ⁴

¹ School of Atmospheric Sciences, Sun Yat-sen University, Zhuhai 519082, China; liuym88@mail.sysu.edu.cn (Y.L.)

² Guangdong Provincial Observation and Research Station for Climate Environment and Air Quality Change in the Pearl River Estuary, Guangzhou 510275, China

³ Southern Marine Science and Engineering Guangdong Laboratory (Zhuhai), Zhuhai 519082, China

⁴ Guangzhou Climate and Agrometeorology Center, Guangzhou 511430, China

⁵ Institute of Tropical and Marine Meteorology, China Meteorological Administration, Guangzhou 510640, China

⁶ Department of Civil and Environmental Engineering, Northeastern University, Boston, MA 02115, USA

⁷ Guangdong Ecological Meteorology Center, Guangzhou 510640, China

⁸ Hong Kong Observatory, Hong Kong 999077, China

* Correspondence: shchong@mail3.sysu.edu.cn

Abstract: Based on morphological methods, MODIS satellite remote sensing data were used to establish a dataset of the local roughness length (Z_0) of vegetation-covered surfaces in Guangdong Province. The local Z_0 was used to update the mesoscale Weather Research and Forecasting (WRF) model in order to quantitatively evaluate its impact on the thermodynamic environment of vegetation-covered surfaces. The specific results are as follows: evergreen broad-leaved forests showed the largest average Z_0 values at 1.27 m (spring), 1.15 m (summer), 1.03 m (autumn), and 1.15 m (winter); the average Z_0 values of mixed forests ranged from 0.90 to 1.20 m; and those for cropland-covered surfaces ranged from 0.17 to 0.20 m. The Z_0 values of individual vegetation coverage types all exhibited relatively high values in spring and low values in autumn, and the default Z_0 corresponding to specific vegetation-covered surfaces was significantly underestimated in the WRF model. Modifying the default Z_0 of surfaces underlying evergreen broad-leaved forests, mixed forests, and croplands in the model induced only relatively small changes (<1%) in their 2 m temperature, relative humidity, skin surface temperature, and the planetary boundary layer height. However, the average daily wind speed of surfaces covered by evergreen broad-leaved forests, mixed forests, and croplands was reduced by 0.48 m/s, 0.43 m/s, and 0.26 m/s, respectively, accounting for changes of 12.0%, 11.1%, and 6.5%, respectively.

Keywords: roughness length; vegetation covered surface; WRF model; Guangdong Province



Citation: Liu, Y.; Shen, C.; Chen, X.; Hong, Y.; Fan, Q.; Chan, P.; Wang, C.; Lan, J. Satellite-Based Estimation of Roughness Length over Vegetated Surfaces and Its Utilization in WRF Simulations. *Remote Sens.* **2023**, *15*, 2686. <https://doi.org/10.3390/rs15102686>

Academic Editor: Carmine Serio

Received: 11 March 2023

Revised: 8 May 2023

Accepted: 17 May 2023

Published: 22 May 2023



Copyright: © 2023 by the authors. Licensee MDPI, Basel, Switzerland. This article is an open access article distributed under the terms and conditions of the Creative Commons Attribution (CC BY) license (<https://creativecommons.org/licenses/by/4.0/>).

1. Introduction

Roughness length (Z_0) refers to the height above the zero-plane displacement in the surface boundary layer at which the surface layer wind speed decreases to zero. It not only characterizes the aerodynamic features of the underlying surface, but also becomes an important parameter in the parameterization of atmospheric boundary layer turbulence. The size of Z_0 reflects the land–atmosphere energy and material exchange, transmission intensity, and interactions to a certain extent [1]. In atmospheric numerical models, the magnitude of Z_0 directly affects the calculation of momentum, heat, and mass exchange between the land surface and the lower atmosphere, and thus impacts the meteorological simulation results of the boundary layer [2]. At present, the Z_0 of various vegetation-covered surfaces in different areas varies, ranging from 0 m to 4 m (Table 1). It has become

a key issue in numerical models to consider the comprehensive impact of the Z_0 on various vegetation-covered surfaces [3–5].

In recent years, a series of studies have been conducted worldwide to determine the Z_0 of different areas and various types of underlying surfaces. Many methods have been developed to determine Z_0 , which can be mainly divided into two categories: meteorological and morphological methods. In meteorological methods, based on the Monin–Obukhov similarity theory, an iterative fitting method is used to find the best fit solution according to wind temperature observations at different heights [6]. With the development of vorticity-related observation techniques, single-layer ultrasonic wind temperature fluctuation data can be used to determine Z_0 based on the relationship between surface turbulence characteristics and Z_0 . For example, Rotach [7] proposed the temperature variance method (TVM) to solve Z_0 by measuring temperature fluctuation variance. Martano [8] presented a method using single-layer ultrasonic anemometer data to determine Z_0 . Chen et al. [9] estimated Z_0 based only on the average wind speed and turbulence flux of a single ultrasonic anemometer. In morphological methods, Z_0 is calculated according to the geometric shape and distribution characteristics of roughness elements on the surface [10]. Many previous observations have shown that Z_0 is related to factors such as height, density, shape, and arrangement of roughness elements. Some researchers applied the aforementioned methods to estimate the Z_0 of different areas and surfaces covered by various vegetation types, as shown in Table 1. Worldwide, researchers mostly used meteorological methods based on the Monin–Obukhov similarity theory to estimate the Z_0 of vegetation-covered surfaces. Among them, Lo [11] and Yang and Friedl [12] estimated the Z_0 of underlying surfaces of broad-leaved forests in Canada, as well as broad-leaved forests and coniferous forests in North America, at 0.97 m, 1.81 m, and 1.65 m, respectively. Mikami et al. [13] estimated the Z_0 of surfaces underlying mixed forests in the Kanto Plain of Japan as 1.16 m. Patil [14] evaluated the Z_0 of cropland-covered surfaces in western India to be 0.001–0.45 m. Regarding the estimation of the Z_0 of various types of vegetation-covered surfaces in China, Zhou et al. [15] compared the Z_0 of broad-leaved-forest-covered surfaces in the Changbai Mountains region obtained using various meteorological methods, such as least squares iterative fitting, Newton’s iterative method, TVM, and the method proposed by Martano. Their results showed that except for the Martano method, which underestimated Z_0 , the other three methods produced the same results with values at 1.0–2.0 m. Zhang et al. [16] applied meteorological methods to estimate the Z_0 of surfaces covered by various vegetation types, including forests, croplands, and grasslands in northern China, and obtained values of 0.58 m, 0.23 m, and 0.06 m, respectively. Xing [17] evaluated the Z_0 of different types of vegetation-covered surfaces, including evergreen coniferous forests, evergreen broad-leaved forests, deciduous coniferous forests, deciduous broad-leaved forests, and mixed forests, in China with morphological methods, and obtained values of 1.43–1.53 m, 1.1–1.2 m, 0.5–0.8 m, 0.51–0.77 m, and 1.1–1.35 m, respectively. Liu et al. [18] determined the Z_0 of subtropical evergreen broad-leaved forests in southern China using meteorological methods, and found that it ranges from 1.26 to 2.96 m in winter and from 1.51 to 3.90 m in spring and summer seasons, with slight seasonal variations. In different countries and regions and across various types of vegetation-covered surfaces, significant heterogeneity has been observed in the estimation of Z_0 .

Table 1. Research on the roughness length of different land use types.

Vegetation Type	Method	Study Area	Roughness Length (m)	Literature
Evergreen broad-leaved forest	Meteorological	Camp Borden (Canada)	0.97	Lo [11]
	Meteorological	North America	1.81	Yang and Friedl [12]

Table 1. Cont.

Vegetation Type	Method	Study Area	Roughness Length (m)	Literature
	Meteorological	Changbai Mountains	2.103 ± 0.366 (Fitting)	Zhou et al. [15]
			2.068 ± 0.481 (Newton's iterative method)	
	1.736 ± 0.553 (TVM)			
	0.518 ± 0.649 (Martano's method)			
	Meteorological	Northern China	0.5826	
Meteorological	Zhuhai	1.51–3.90 (spring and summer)	Liu et al. [18]	
	Morphological	China	1.1–1.2	Xing [17]
	Morphological	Beijing	0.6–1.3	Liu et al. [19]
Evergreen needle-leaf forest	Meteorological	North America	1.65	Yang and Friedl [12]
	Morphological	China	1.43–1.53	Xing [17]
Deciduous broad-leaved forest	Morphological	China	0.51–0.77	Xing [17]
Deciduous needleleaf forest	Morphological	China	0.5–0.8	Xing [17]
Mixed forest	Meteorological	Kanto Plain (Japan)	1.16	Mikami et al. [13]
	Morphological	China	1.1–1.35	Xing [17]
Cropland	Meteorological	Western India	0.001–0.45	Patil [14]
	Meteorological	Inner Mongolia	0.21	Mao et al. [20]
	Meteorological	The Loess Plateau	0.017 (spring) 0.062 (summer) 0.065 (autumn) 0.018 (winter)	Zhang et al. [21]
	Meteorological	Northern China	0.2341	Zhang et al. [16]
Grassland	Meteorological	Hebei	0.17–0.41	Ju [22]
	Meteorological	Yuzhong	0.123	Yao et al. [23]
	Meteorological	Maqu area in the upper reaches of the Yellow River	0.035	Li et al. [24]
	Meteorological	Northern China	0.0641	Zhang et al. [16]
	Meteorological	Qinghai	0.014–0.046	Ju [22]
	Meteorological	Yuzhong	0.015	Yao et al. [23]
	Morphological	Northern Tibetan Plateau	0.001–0.043	Sun et al. [25]

Currently, in the default atmospheric numerical model, Weather Research and Forecasting (WRF), Z_0 values are fixed for specific land-use types in the grid of simulated areas: 0.5 m for evergreen broad-leaved forests in summer and winter, 0.5 m and 0.2 m for mixed forests in summer and winter, respectively, and 0.15 m and 0.05 m for croplands in summer and winter, respectively. Compared with estimated Z_0 values reported in the literature (Table 1), the default Z_0 values of major vegetation-covered surfaces in the WRF model are underestimated, and do not accurately represent the Z_0 of the underlying surfaces in various regions. In recent years, some researchers have attempted to apply the calculated Z_0 to land surface models in order to reflect the actual Z_0 values. Li et al. [24] and Lu et al. [26] used turbulence observation data from the source regions of the Yellow River and Inner Mongolia to estimate the Z_0 of grassland- and desert-covered surfaces. The data were applied to the land surface model CoLM to improve parameters, through which model simulations could be significantly improved in terms of sensible heat flux, latent heat flux, soil temperature, and net surface radiation. Chen and Lv [27] substituted the calculated Z_0 in the Noah land surface model and found that the simulated surface temperature and sensible heat flux in Gobi and desert areas were more accurate than those based on the

original Z_0 , and it significantly improved the ability of the model in simulating the surfaces of Gobi and other special areas. Zheng et al. [28] and Huang et al. [29] evaluated the default and updated dynamic and thermal Z_0 parameterizations in the land surface model Noah for alpine grasslands in the Tibetan Plateau and Yangtze River Delta, respectively. The results show that the accuracy of the simulated sensible heat flux, latent heat flux, surface temperature, and soil temperature could be substantially enhanced by the updated scheme. Shen et al. [30] revised the default Z_0 value of the Pearl River Delta region in the WRF–Chem model based on the actual calculated Z_0 value of various underlying surfaces from the literature. They found that the simulation performance of the model over the Pearl River Delta region could be improved by updating Z_0 , which resulted in the most remarkable reduction in the wind speed over the urban underlying surface, accounting for a reduction of about 26%. In summary, the Z_0 in a model has a significant impact on the meteorological field simulation, and its accuracy is very important for improving the performance of land surface models and mesoscale meteorological models.

At present, most of the research on the Z_0 in land surface models or atmospheric numerical models involves the estimation of Z_0 based on single-point observation data of one or several types of underlying surfaces, which are then used to represent the Z_0 of the corresponding underlying surface type in the area for the improvement and evaluation of the models. However, studies on Z_0 estimation and model improvement at regional scales are relatively rare. As vegetation types and growth cycles vary across the globe, the spatial and temporal distribution of Z_0 will show remarkable regional variations.

Taking Guangdong Province as an example, we estimated the Z_0 values over the vegetated surfaces and incorporated these updated values into the WRF simulation. Morphological methods that support the estimation and investigation of regional Z_0 were selected. Satellite remote sensing data inversion was used to calculate the Z_0 of the main types of vegetation-covered surfaces in Guangdong Province, and the estimated values were applied to improve the WRF model and evaluate its impact on the thermodynamic environment of the surface boundary layer of the vegetation-covered surfaces.

2. Methodology

2.1. Research Data

According to the Guangdong Climate Bulletin in 2017 issued by the Climate Center of Guangdong Meteorological Bureau, the year 2017 was a normal year in Guangdong in terms of climate, with slightly higher temperature and comparable precipitation and sunlight duration compared with previous years. The data used here include the 2017 Moderate Resolution Imaging Spectroradiometer (MODIS) combined Leaf Area Index (LAI) and Fraction of Photosynthetically Active Radiation (FPAR) Version 6 product (MOD15A2H) and the 2013 Terra and Aqua combined MODIS Land Cover Type (MCD12Q1) version 6 data product. The MOD15A2H data is the latest level 4 LAI product released by the National Aeronautics and Space Administration (NASA) in 2015 and is available at <https://search.earthdata.nasa.gov/search> (accessed on 20 May 2023). Its spatial resolution is 500 m, and an 8-day composite data file in HDF format is formed every 8 days. There are 46 files per year, and each file specifically includes the LAI and FPAR data layers. MCD12Q1 is the Terra and Aqua combined MODIS land cover type version 6 data product. It provides global land cover types every year with a spatial resolution of 500 m. There are 6 different classification schemes in this product, among which the International Geosphere Biosphere Programme (IGBP) was selected in this study. This scheme contains 17 types of specific classifications (Figure 1).

2.2. Study Area

Guangdong Province is located in the southernmost part of Mainland China, with an area of 179,725 km². The geomorphological characteristics of Guangdong Province are dominated by mountainous and hilly terrain, whereas the topography of the Pearl River Delta region (the centre of Guangdong Province) is characterized by low-lying

plains (Figure S1). It is surrounded by mountains to the north, west, and east. It enjoys a subtropical monsoon climate with many types of vegetation covering in a broad area, including evergreen broad-leaved forests, mixed forests, croplands, and grasslands. Figure 1 shows the distribution map of IGBP land cover types in Guangdong. The area proportions of various land cover types within the administrative boundary of Guangdong Province are shown in Table 2. Here, mixed forest refers to the forest composed of two or more types of trees. In Guangdong Province, it is mainly the mixed needle and broad-leaved forest. For the cropland, rice is the main crop that occupies the largest proportion of cropland area in Guangdong Province in 2017, according to the Guangdong Statistical Yearbook on Agriculture [31]. Table 2 shows that evergreen broad-leaved forests occupy the highest proportion of area in Guangdong Province, accounting for more than one-third (37.40%) of the area of Guangdong Province, followed by woody savanna (16.51%), cropland/natural vegetation mosaic (16.18%), and croplands (12.53%), all of which are above 10%. In addition, mixed forests and urban and built-up land have relatively high ratios at 7.67% and 4.31%, respectively. In total, these types account for 90.29% of the total area of Guangdong Province. In this study, we focus on three major vegetation types which occupy a relatively high proportion of area in Guangdong Province, including evergreen broad-leaved forests, mixed forests, and cropland.

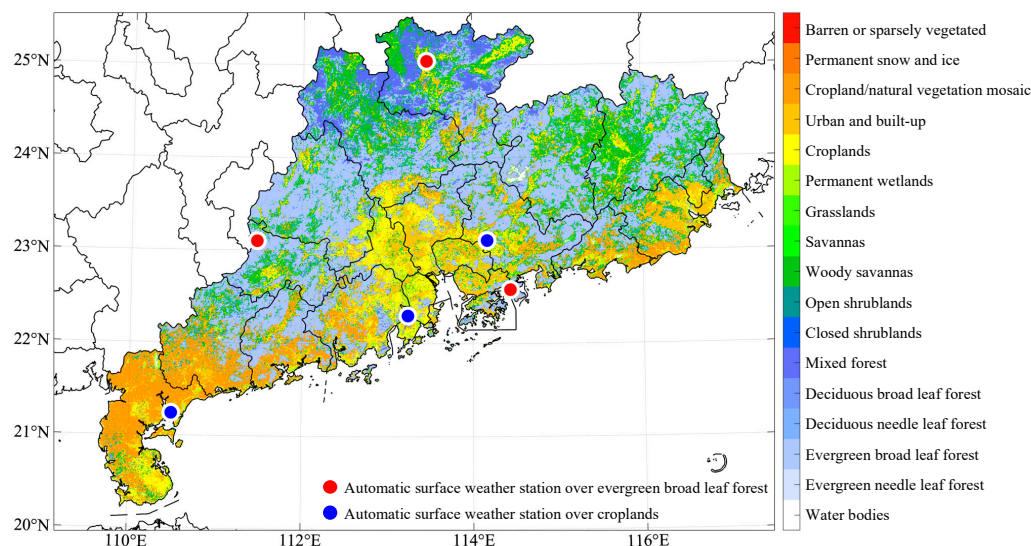


Figure 1. Spatial distribution of IGBP land cover types in Guangdong Province. The red and blue dots are the locations of the automatic surface weather stations over evergreen broad-leaved forest and croplands, respectively.

Table 2. Proportions of major IGBP land cover types in Guangdong Province.

Rank	Land Cover Type	Proportion (%)
1	Evergreen broad-leaved forest	37.40
2	Woody savannas	16.51
3	Cropland/natural vegetation mosaic	16.18
4	Croplands	12.53
5	Mixed forest	7.67
6	Urban and built-up	4.31
7	Permanent wetlands	2.27
8	Water bodies	1.76
9	Others	1.37

2.3. Introduction of Morphological Estimation Methods

As vegetation is an important component of the ecosystem and the vegetation coverage of Guangdong Province accounts for more than half of the province, it is very important to

accurately describe the Z_0 of the vegetation-covered surfaces. Raupach [32,33] proposed a semi-empirical model to estimate the vegetation Z_0 through a wind tunnel experimental study of a cylindrical array. The calculation equations are as follows:

$$\frac{Z_0}{h} = \left(1.0 - \frac{Z_d}{h}\right) \exp\left(-k \frac{U}{u_*} + \varphi_h\right) \quad (1)$$

$$\frac{Z_d}{h} = 1.0 - \frac{1.0 - \exp\left(-\left(C_{d1} \times 2\lambda_f\right)^{0.5}\right)}{\left(C_{d1} \times 2\lambda_f\right)^{0.5}} = \left(\frac{\beta\Lambda}{2 + \beta\Lambda}\right) \left(1 - \alpha r^{-1} \Lambda^{-0.5}\right) \quad (2)$$

$$\frac{U}{u_*} = r = \left(C_s + C_R \lambda_f\right)^{0.5} \times \exp\left(\frac{c\lambda_{fr}}{2}\right) \quad (3)$$

where $\frac{Z_0}{h}$ is the normalized roughness length; Z_d is the height of the zero-plane displacement; $\frac{Z_d}{h}$ is the normalized height of the zero-plane displacement; h is the height of the vegetation; φ_h is the influence function of the rough layer, with a value of 0.193; C_{d1} is the empirical coefficient, with a value of 7.5; k is the Von Karman constant, with a value of 0.4; C_s is the surface resistance coefficient, with a value of 0.003; C_R is the resistance coefficient of roughness elements; U is the wind speed; u_* is the friction speed; λ_f is the frontal area index of vegetation, $\lambda_f = \Lambda/2$; Λ is the vegetation canopy area index; c is the shading coefficient of roughness elements; $\alpha = C_{d1} \left(\frac{2b}{h}\right)^{0.5}$; and $\beta = \frac{C_R}{C_s}$.

When Λ is greater than Λ_{max} , the airflow starts to pass through the vegetation surface instead of through the vegetation, so $\frac{u_*}{U}$ will no longer increase with the increase of Λ or λ_f , with the fixed value of $\left(\frac{u_*}{U}\right)_{max}$.

Through the above equations, when estimating Z_0 , the vegetation height and vegetation canopy area index are input variables, while C_R , C_s , α , c , $\left(\frac{u_*}{U}\right)_{max}$, φ_h , and Λ_{max} are the required parameters. Based on the Raupach [32,33] method, Jasinski et al. [34] used field observation data to establish the aforementioned parameters of each vegetation-covered surface according to the IGBP surface-coverage types, among which $\varphi_h = 0.193$, $C_s = 0.003$, and the remaining 5 parameters are assigned according to different vegetation types, as shown in Table S1.

For the vegetation canopy area index Λ , the equations defined by Zeng et al. [35] were used in this study, which are as follows:

$$\Lambda \cong I_s + I_g \quad (4)$$

$$I_s^n = \max\left(\left(\alpha I_s^{n-1} + \max\left(I_g^{n-1} - I_s^n, 0\right)\right), I_{s,min}\right) \quad (5)$$

In the above equations, I_g is the LAI, I_s is the dry LAI, I_s^n is the dead LAI of the n th month, $I_{s,min}$ is the monthly minimum dead LAI of different vegetation types, and $1-\alpha$ is the removal rate of dead leaves. Different values are assigned to $I_{s,min}$, and α for various vegetation types. According to the values of these two items for different IGBP surface cover types given by Zeng et al. [35], as shown in Table S2, $I_{s,min}$ and α of different vegetation types in the study area can be obtained. The LAI I_g can be directly acquired from the LAI data of the MOD15A2H product.

Regarding vegetation height, in this study, the heights of different vegetation types were mainly obtained from the literature [17,19,36]. The heights obtained were 18 m for evergreen broad-leaved forests, 15 m for mixed forests, 6.6 m for woody savannas, 1.5 m for croplands, and 4.1 m for cropland/natural vegetation mosaic.

The method for estimating the Z_0 of vegetation-covered surfaces involves pre-treatment processes such as reprojection and data stitching of the 2017 MOD15A2H data and 2013 MCD12Q1 data to determine the LAI and IGBP land cover types with a 500 m horizontal resolution using the MODIS data-processing software MRT (MODIS Reprojection Tools).

The normalized Z_0 was obtained according to the above-mentioned method, different vegetation heights were acquired from the literature, and, finally, the Z_0 of the main vegetation-covered surfaces was obtained.

3. Result and Discussion

3.1. Temporal and Spatial Analysis of Roughness Length

Based on the IGBP land cover types, the 2017 MOD15A2H data were processed to obtain the spatial distribution of the average vegetation canopy area index for representative months of different seasons in Guangdong Province with 500 m horizontal resolution, as shown in Figure 2. It indicates that the vegetation canopy area index of the central area of the Pearl River Delta (Southern Guangzhou, Foshan, Zhongshan, Dongguan, Shenzhen, and Zhuhai) was the lowest compared with other areas in each month, and the main vegetation type in this area is cropland. Croplands and natural vegetation mosaic are the main types in southern Guangdong (Zhanjiang and Maoming), where the vegetation canopy area index of each month is also significantly lower than that of areas in northern and western Guangdong, with the lowest in spring (April) and the highest in autumn (October). The vegetation canopy area index of the widely distributed evergreen broad-leaved forest was significantly higher than that of other land cover types. It was generally above 48 in October, and the lowest value occurred in April, ranging from 30 to 40. It was significantly different from that of the broad-leaved forest in the north. Liu et al. [19] applied the same method to estimate the vegetation canopy area index of broad-leaved forests in Beijing and found that the vegetation canopy area index in winter was relatively low and the highest value was in summer.

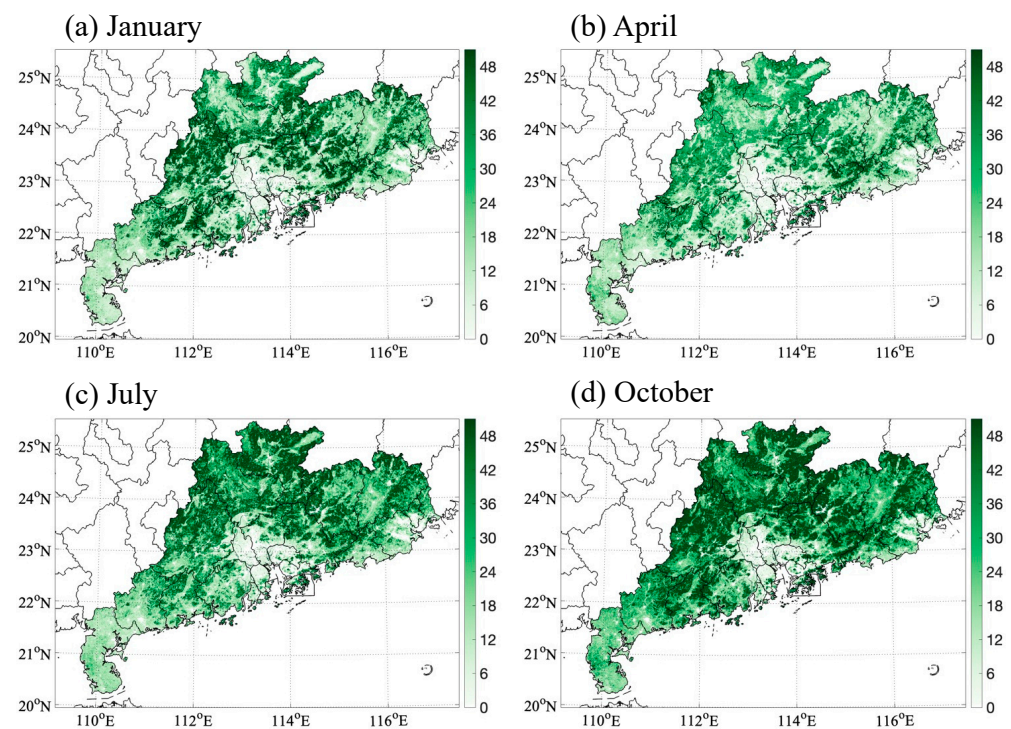


Figure 2. Spatial distribution of vegetation canopy area index (dimensionless) in different months in Guangdong Province in 2017.

According to the estimation method, the distribution of the average normalized Z_0 in the representative months of each season in 2017 in Guangdong Province was obtained, as shown in Figure 3. The figure shows that croplands had a relatively high normalized Z_0 in the central area of the Pearl River Delta, which was above 0.12 in every month. It was followed by cropland and natural vegetation mosaics in southern Guangdong (Zhanjiang and Maoming), with the highest normalized Z_0 of above 0.11 in April. Evergreen broad-

leaved forests showed the lowest normalized Z_0 in Guangdong Province, especially in October, at about 0.06. From the distribution maps of the average Z_0 of the main underlying surfaces for representative months in different seasons of 2017 in Guangdong Province (Figure 4), it can be observed that evergreen broad-leaved forests and mixed forests in northern and western Guangdong had higher Z_0 , reaching the highest in April (over 1 m) and lowest in October. The Z_0 of croplands in the central area of the Pearl River Delta was low.

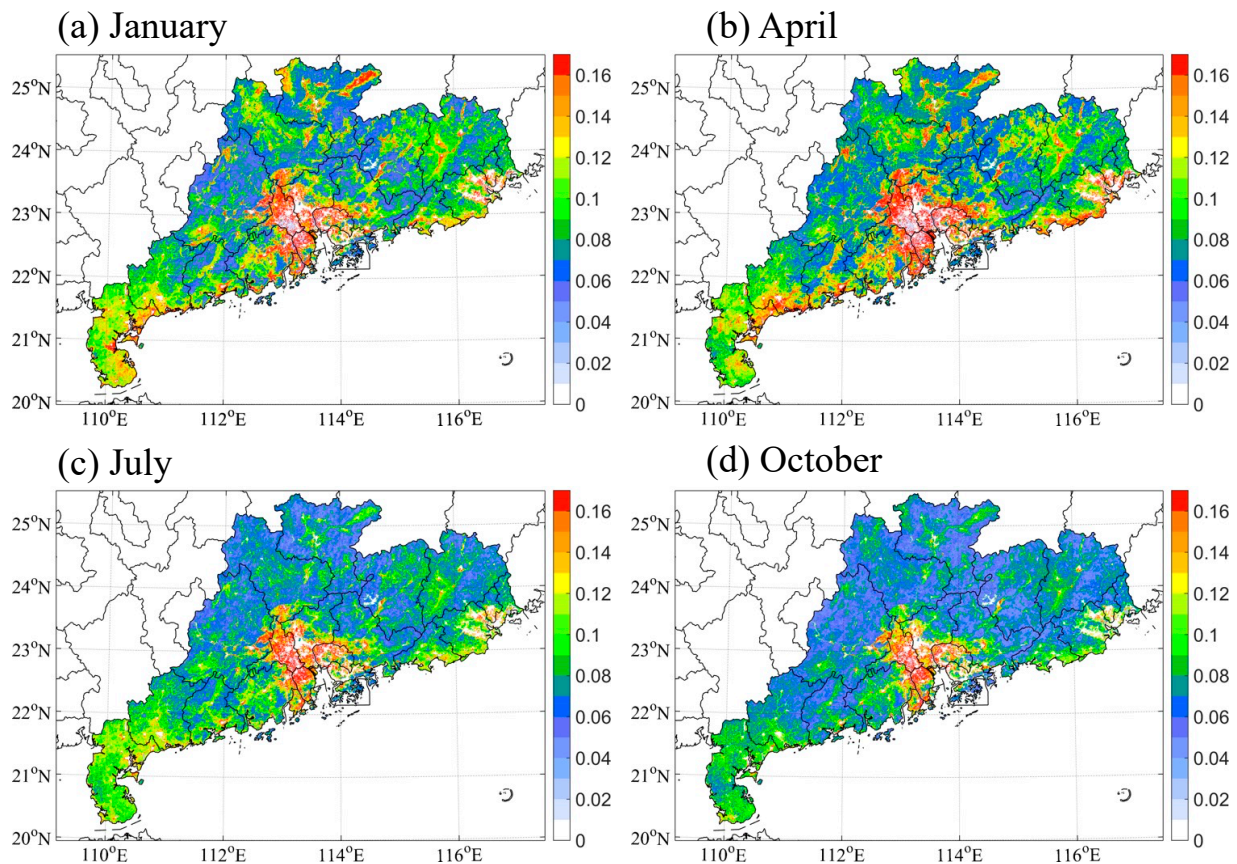


Figure 3. Distribution of average normalized roughness length (dimensionless) in different months in Guangdong Province in 2017.

Figure 5 shows the monthly changes of vegetation canopy area index, normalized Z_0 , and Z_0 of major single vegetation types in Guangdong Province in 2017, including evergreen broad-leaved forests, mixed forests, and cropland. The vegetation canopy area index of evergreen broad-leaved forests was the highest in all months, with values exceeding 30. For this vegetation type, the lowest vegetation canopy area index was observed in March and April (about 34–35), and the highest in September and October (above 50). Mixed forests showed the second highest values, and croplands showed the lowest values with a substantially lower magnitude of monthly change compared to that of evergreen broad-leaved forests and mixed forests. Regarding the normalized Z_0 , croplands showed the highest values, reaching above 0.1 in all months. The highest value (0.14) appeared from February to April, after which it dropped to the lowest level (0.11) from September to October. This vegetation cover type exhibited remarkable monthly differences. Evergreen broad-leaved forests and mixed forests exhibited low normalized Z_0 , with the highest values in March and April and a small range of monthly variations between 0.05 and 0.08. In terms of Z_0 , evergreen broad-leaved forests showed the highest values, followed by mixed forests at above 0.9 m in all months. The main reason is that the vegetation height of these two types is significantly higher than that of other types. Croplands had the lowest roughness length, ranging between 0.16 and 0.2 m, with a small magnitude of changes.

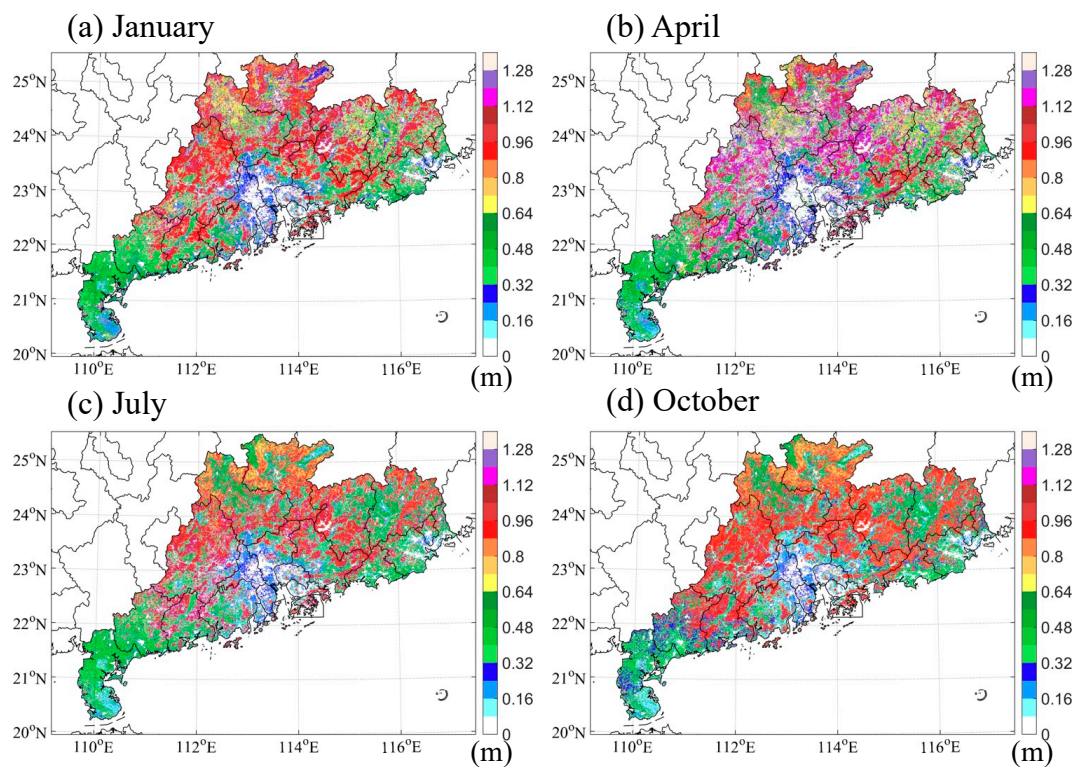


Figure 4. Distribution of average roughness length (of main underlying surface types) in different months in Guangdong Province in 2017.

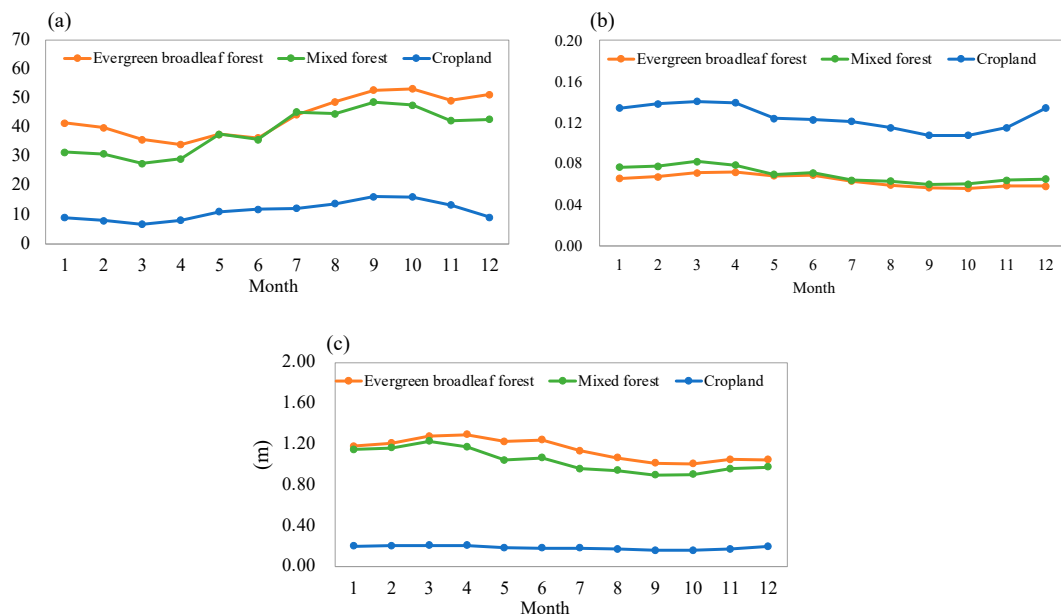


Figure 5. Monthly variation of vegetation canopy area index (a), normalized roughness length (b), and roughness length (c) of main vegetation types in 2017.

According to Z_0 values of the major single vegetation types in different seasons of 2017 in Guangdong Province (Table 3), the vegetation types can be arranged in the following order with Z_0 from high to low: evergreen broad-leaved forests, mixed forests, and cropland. The seasonal average Z_0 values of evergreen broad-leaved forests were 1.27 m (spring), 1.15 m (summer), 1.03 m (autumn), and 1.15 m (winter), which are all above 1 m. The seasonal average Z_0 values of mixed forests were slightly lower than those of evergreen broad-leaved forests, ranging from 0.9 to 1.2 m. Croplands in the central region of the Pearl

River Delta showed the lowest Z_0 values, and their seasonal averages ranged between 0.17 and 0.2 m, with small variations. The Z_0 of all individual vegetation cover types showed relatively high values in spring and low values in autumn.

Table 3. Roughness length values of main vegetation types in different seasons in Guangdong Province in 2017.

Roughness Length (m)	Evergreen Broad-Leaved Forest	Mixed Forest	Cropland
Spring	1.27	1.15	0.20
Summer	1.15	0.99	0.18
Autumn	1.03	0.92	0.17
Winter	1.15	1.10	0.20

3.2. Improvement of Roughness Length in Models

Surfaces underlying different land-use types in the WRF model have fixed Z_0 values for the summer and winter settings. The default and estimated Z_0 values of the three vegetation cover types in summer and winter were compared, and details are presented in Table 4. The default Z_0 of evergreen broad-leaved forests is 0.5 m for both seasons, while the estimated value for Guangdong Province was 1.15 m in summer and winter, which is significantly higher than the default value. The default Z_0 values of the mixed forest are 0.5 m and 0.2 m in summer and winter, respectively, showing a remarkable difference, while the estimated values for Guangdong Province were 0.99 m and 1.10 m in summer and winter, respectively, which are higher than the default values and exhibit a relatively small difference. This can be attributed to the relatively warm winter in Guangdong Province, which allows vegetation to flourish. Therefore, the vegetation canopy area index in winter varies only slightly from that in summer, resulting in a relatively small difference in the corresponding Z_0 . For croplands, the default Z_0 values are 0.15 m and 0.05 m in summer and winter, respectively, while the estimated values for Guangdong were 0.18 m and 0.20 m in summer and winter, respectively, which are significantly higher than the default values. This comparison shows that the default values of individual vegetation types significantly differ from the estimated Z_0 values for Guangdong Province based on MODIS data, with the estimated values being substantially higher than the default values, especially in winter. In general, the default roughness lengths of the models in summer are higher than those in winter. However, owing to Guangdong's unique geographical location where distinct seasons are not observed, there is no noticeable difference in vegetation growth and the estimated Z_0 does not significantly change between summer and winter. In addition, as shown in Table 1, the estimated Z_0 for evergreen broad-leaved forests, mixed forests, and croplands in China from the literature ranged from 0.52 to 3.90 m, from 1.10 to 1.35 m, and from 0.21 to 0.23 m, respectively. The estimated Z_0 values for these three vegetation types in this study are comparable with these values, while the default settings in the WRF model are underestimated obviously. We thus consider that the Z_0 values we estimated are more reliable than the model-default ones. This suggests that it is necessary to incorporate these updated Z_0 values into the WRF model.

Table 4. Comparison between the default and estimated values of roughness length in the main underlying surface types. The estimated Z_0 values in China from the literature (Table 1) are also provided for comparison.

Type of Vegetation Cover	Default Model Value		Estimated Value in Guangdong Province		Values in China from the Literature (Table 1)
	Summer	Winter	Summer	Winter	
Evergreen broad-leaved forest	0.5	0.5	1.15	1.15	0.52–3.90
Mixed forest	0.5	0.2	0.99	1.10	1.10–1.35
Cropland	0.15	0.05	0.18	0.20	0.21–0.23

3.3. Assessment of the Impact of Roughness Length Improvement on the Near-Surface Thermodynamic Field

3.3.1. Simulation Scheme Settings

The WRF model version 3.8.1 [37] used in this study applied a triple-domain configuration with the centre point set in Guangzhou (23.3°N, 113.5°E), using the LAMBERT projection method. A total of 30 layers were set up vertically, and the air pressure at the top of the model was 50 hPa. The domain used grids of 160×181 , 181×190 , and 301×283 , with grid intervals of 27 km, 9 km, and 3 km, respectively, covering the entire Guangdong Province. The simulated area is shown in Figure 6, with initial meteorological and boundary conditions from the $1^\circ \times 1^\circ$ NCEP FNL global reanalysis data, which were extrapolated into the simulation area. The land-use data for the study area were obtained from GLC2009 [38], which are more applicable to the Guangdong area. The physical parameterization schemes used in the simulation included the new Goddard shortwave radiation scheme, RRTM longwave radiation scheme, Lin microphysics scheme, YSU boundary layer parameterization scheme, Noah land surface process scheme, and Kain–Fritsch cumulus scheme, among which the cumulus scheme was used only for the first two grids.

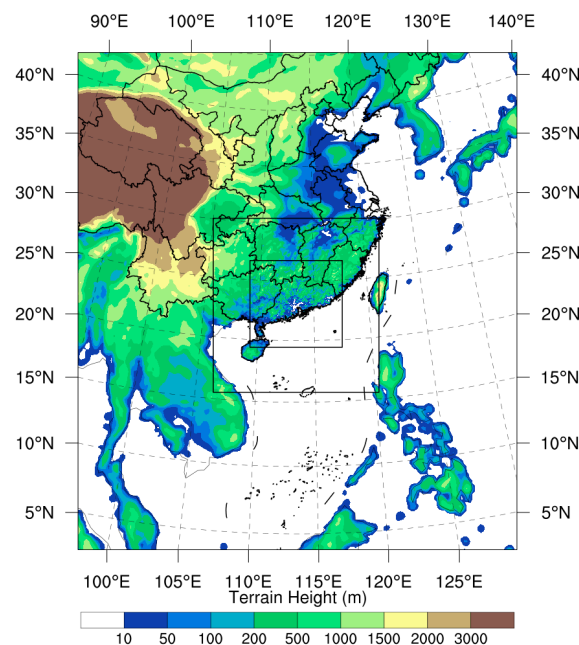


Figure 6. Three nested domains in the WRF simulation.

The simulation time was from 00:00 on 30 October 2017 to 00:00 on 1 December (Universal Time). Considering the spin-up time, the research period was set from 00:00 on 1 November 2017 to 23:00 on 30 November (local standard time). November is a typical dry and cold month in Guangdong Province. As shown in Figure 5a, the vegetation canopy area index in this month is relatively higher than in other months. In this study, two modelling experiments were designed regarding different Z_0 values. The base scheme uses the model-default Z_0 values for surfaces underlying three types of vegetation (evergreen broad-leaved forests, mixed forests, and croplands), while the case scheme substitutes it with the estimated one for Guangdong Province (Table 4). Quantitative analysis of the Z_0 between the case and base was used to evaluate the impact on the thermal and dynamic environment of vegetation-covered surfaces.

3.3.2. Assessment of Impact on the Thermodynamic Field

The impact of Z_0 improvement on relative changes in the daytime (8:00–16:00) and nighttime (17:00–7:00) meteorological elements was evaluated for all surfaces underlying evergreen broad-leaved forests, mixed forests, and croplands in Guangdong Province con-

sidering thermodynamic and dynamic meteorological elements, such as 2 m temperature (T2), relative humidity (RH), skin surface temperature (TSK), ground heat flux (GRD), sensible heat flux (HFX), planetary boundary layer height (PBLH), and 10 m wind speed (WS), as shown in Figure 7. The effects of Z_0 change on T2, RH, TSK, and PBLH were relatively small, with change rates of less than 1% for both daytime and nighttime values. Meteorological elements that are more sensitive to the updated Z_0 values of vegetation-covered surfaces include WS, followed by GRD and HFX. WS of the surface underlying evergreen broad-leaved forests and mixed forests decreased by more than 10%, and that of croplands decreased by about 5–7%, mainly attributable to the different degrees of Z_0 change. After redefining Z_0 based on the vegetation coverage in the land surface model, the Z_0 values of vegetation-covered surfaces changed from the model defaults of 0.33 m, 0.30 m, and 0.18 m to the estimated values of 0.67 m, 0.58 m, and 0.25 m, respectively. The extent of Z_0 increase was significantly greater for evergreen broad-leaved-forest- and mixed-forest-covered surfaces than for cropland-covered surfaces. The updated Z_0 also resulted in a 1–2% reduction in the daytime and nighttime GRD of surfaces underlying evergreen broad-leaved forests and mixed forests during the day and night, while HFX increased by less than 1% during the day and decreased by 2–4% at night.

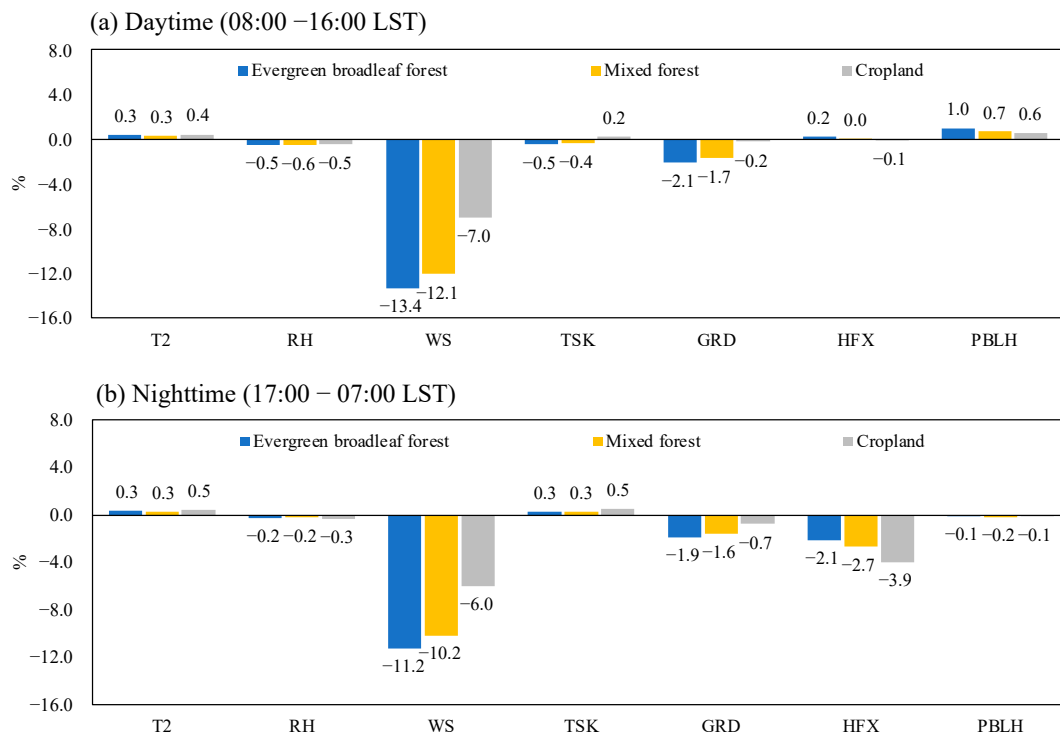


Figure 7. Effects of updated Z_0 on meteorological elements in evergreen broad-leaved forest, mixed forest, and cropland land-use types during the daytime and nighttime in November; daytime: 8:00–16:00; night-time: 17:00–7:00; change rate: $(\text{case} - \text{base}) / \text{base} \times 100$. LST is the local standard time.

The effect of changes in Z_0 on the relatively sensitive meteorological elements of evergreen broad-leaved-forest-, mixed-forest-, and cropland-covered surfaces was further analysed. Figure 8 shows the daily variation of the average thermodynamic meteorological elements in November of the case scheme compared with the base scheme. The effect of the Z_0 change on TSK, GRD, and HFX was significantly greater for evergreen broad-leaved-forest- and mixed-forest-covered surfaces than for cropland-covered surfaces. In addition, the impact of Z_0 change on the thermal field during the day was slightly greater than that at night. TSK of evergreen-broad-leaved-forest- and mixed-forest-covered surfaces decreased by 0.12 °C and 0.10 °C during the day, respectively, and increased by 0.06 °C and 0.05 °C at night, respectively. Because heat is transferred from the land surface to the soil during the

day, GRD was negative. At night, heat is transferred from the soil to the surface, and thus, GRD is positive. During the day, the average GRD of evergreen-broad-leaved-forest- and mixed-forest-covered surfaces decreased by 0.76 W/m^2 and 0.62 W/m^2 , respectively. The most substantial decrease occurred at noon (about 2 W/m^2), and GRD was also slightly decreased at night. HFX was positive during the day, when heat is transferred from the land surface to the atmosphere. In surfaces underlying evergreen broad-leaved forests and mixed forests, HFX increased significantly by about $2\text{--}3 \text{ W/m}^2$ and 2 W/m^2 in the afternoon (12:00–14:00 LST), respectively, while night heat flux decreased by 0.28 W/m^2 and 0.33 W/m^2 , respectively. The above phenomenon can be attributed to the increase of Z_0 causing more remarkable heat turbulence exchange near the surface layer, which is conducive to vertical heat flux transportation, such that more heat is transferred from the land surface to the atmosphere. HFX increases during the day, and the surface temperature decreases. The amount of heat transferred to the soil is reduced, and GRD declines. As the amount of stored heat during the day is reduced, the heat released at night is reduced accordingly, and so is the surface temperature at night.

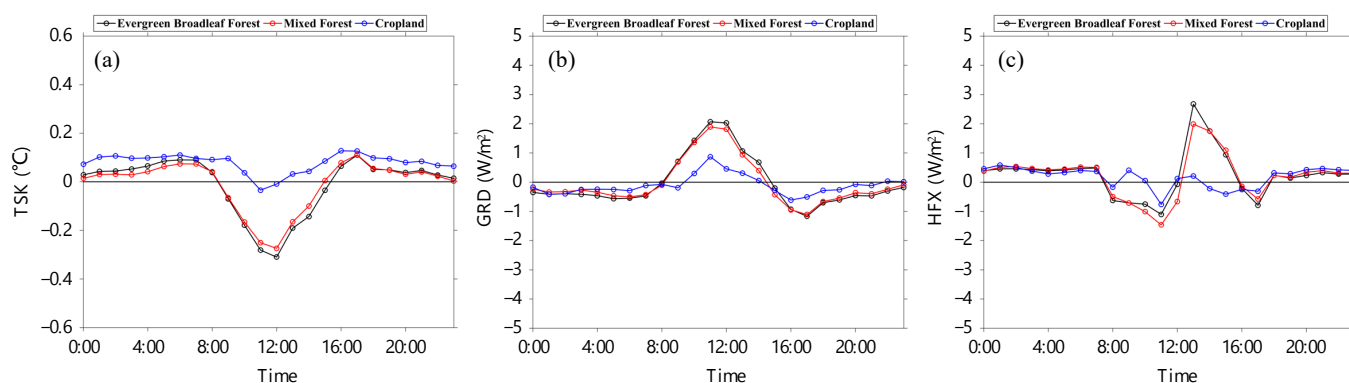


Figure 8. Effects of updated Z_0 on the daily variation of (a) skin surface temperature (TSK), (b) ground heat flux (GRD), and (c) sensible heat flux (HFX) in evergreen broad-leaved forest, mixed forest, and cropland land-use types in November.

WS is the most important meteorological factor affected by the updated Z_0 values in the WRF model. We compared the observed WS with the observations from six automatic surface weather stations in Guangdong. The locations of these sites are shown in Figure 1. Three sites are located over the underlying surface of evergreen broad-leaved forest, and the other three sites are located over those of cropland. We then averaged the results of these sites to represent the model performance at these two vegetation covers. Four statistical parameters were used to evaluate the simulated value against the observation, including mean bias (MB), mean absolute error (MAE), root mean square error (RMSE), and correlation coefficient (R). Their calculation equations can be found in the study by Shen et al. [39]. Table 5 presents these statistical results. It shows that the base experiment with the default Z_0 setting overestimates the wind speed. After the update of the Z_0 , the case experiment lowers the MBs of wind speed both for the evergreen broad-leaved forest and croplands, which suggests that the updated Z_0 in the case scheme can yield better WS simulations.

Table 5. Statistical comparison of the simulated and observed 10 m wind speed (WS, m/s) at the main underlying surfaces.

Land Cover Type	Sites	MB		MAE		RMSE		R	
		Base	Case	Base	Case	Base	Case	Base	Case
Evergreen broad-leaved forest	3	1.51	1.04	1.80	1.43	2.21	1.75	0.29	0.27
Croplands	3	1.64	1.47	1.82	1.69	2.24	2.06	0.37	0.36

Figure 9 shows the daily variation of the average WS in November after the Z_0 update. For the evergreen-broad-leaved-forest-, mixed-forest-, and cropland-covered surfaces, the simulated WS values reduced from 3.99 m/s (base) to 3.51 m/s (case), from 3.89 m/s (base) to 3.46 m/s (case), and from 3.99 m/s (base) to 3.73 m/s (case), respectively. This shows that the increase in Z_0 decreased the daily average WS of these three vegetated surfaces by 0.48 m/s, 0.43 m/s, and 0.26 m/s, respectively, accounting for 12.0%, 11.1%, and 6.5%, respectively. These changes can be attributed to the update of Z_0 values from 0.33 m, 0.30 m, and 0.18 m to 0.67 m, 0.58 m, and 0.25 m, respectively. The increased surface friction resulted in a significant reduction in wind speed. The reduction of the average daily WS was higher for evergreen-broad-leaved-forest- and mixed-forest-covered surfaces than for cropland-covered surfaces.

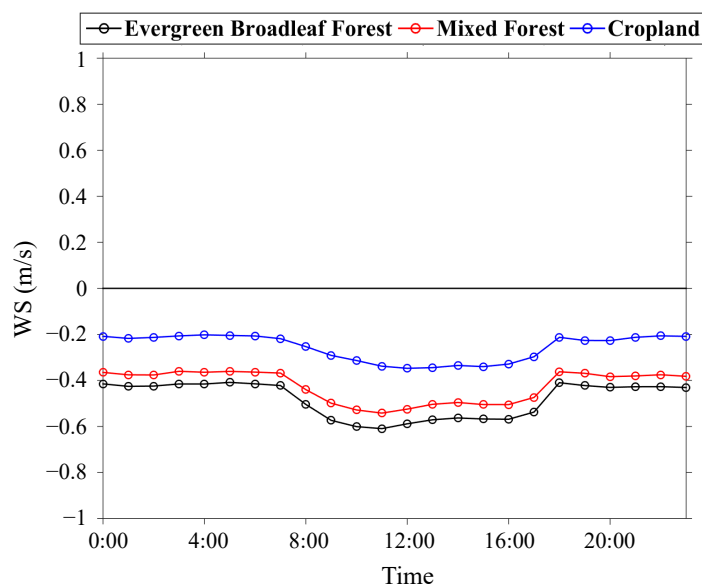


Figure 9. Effects of updated Z_0 on the daily variation of the 10 m wind speed (WS) in evergreen broad-leaved forest, mixed forest, and cropland land-use types in November.

4. Conclusions

Based on morphological methods, MODIS satellite data were used to estimate the Z_0 of the vegetation-covered surfaces in Guangdong Province in 2017, and its spatial and temporal distribution characteristics were examined. The default Z_0 values of the major individual vegetation types in the WRF model were updated to quantitatively analyse their impact on the atmospheric thermodynamic environment of the vegetation-covered surfaces. The specific conclusions are as follows:

1. Vegetation-covered surfaces in Guangdong Province can be listed in the descending order of Z_0 as evergreen broad-leaved forest, mixed forest, and cropland. The average Z_0 values of evergreen broad-leaved forests in each season were 1.27 m, 1.15 m, 1.03 m, and 1.15 m, which are all above 1 m. The average Z_0 of mixed forests in each season ranged between 0.9 and 1.2 m. The Z_0 of croplands was the lowest, with average values between 0.17 and 0.2 m. The roughness length was higher in spring and lower in autumn for all individual vegetation cover types.
2. The estimated values of Z_0 for each vegetation type in Guangdong Province were quite different from the default values of the model, with the estimated values being significantly higher than the default values, especially in winter. The default Z_0 of evergreen broad-leaved forests in the model is 0.5 m for all seasons, but the estimated value for Guangdong was 1.15 m for both the summer and winter seasons. The default Z_0 values of mixed forests in the model are 0.5 m in summer and 0.2 m in winter, but the estimated values for Guangdong were 0.99 m and 1.10 m, respectively, showing a slight seasonal difference. The default Z_0 values of croplands in the model

are 0.15 m and 0.05 m for summer and winter, respectively, but the estimated values for Guangdong were 0.18 m for summer and 0.20 m for winter.

3. The default Z_0 values in the model were revised for the surfaces underlying evergreen broad-leaved forests, mixed forests, and croplands. The updated Z_0 was found to have a slightly greater impact on meteorological elements during the day than at night. The change of Z_0 has a relatively small effect on T2, RH, TSK, and PBLH of each underlying surface, with all changes below 1%. The updated (increased) Z_0 resulted in a decrease in daily average WS by 0.48 m/s, 0.43 m/s, and 0.26 m/s for surfaces underlying evergreen broad-leaved forests, mixed forests, and croplands, respectively, accounting for changes of 12.0%, 11.1%, and 6.5%, respectively. The updated Z_0 also resulted in a 1–2% reduction in the daytime and nighttime GRD of surfaces underlying evergreen broad-leaved forests and mixed forests, and a 1% increase and 2–4% decrease in HFX during the day and night, respectively.
4. The overestimation of wind speed has long been a concern in atmospheric modelling [40–43]. The increase in Z_0 over vegetated surfaces that is parametrized in the land surface model can partly reduce the overestimation of wind speed. The approach of this study can be extended to other regions to improve the simulations and forecasts using the atmospheric numerical model. Such improvement can further yield better simulation results in the modelling of air quality and climate. The weakness of this study is that the current vegetation height to derive Z_0 over vegetated surfaces is based on the literature values. We expect to collect actual vegetation heights for further estimation in the future.

Supplementary Materials: The following supporting information can be downloaded at: <https://www.mdpi.com/article/10.3390/rs15102686/s1>, Figure S1: Geomorphological map of Guangdong Province, China; Table S1: Parameters of different land (vegetation) cover types in the estimation model (Jasinski et al., 2005 [34]); Table S2: Values of $I_{s,min}$ and α in different land (vegetation) cover types (Zeng et al., 2002 [35]).

Author Contributions: Conceptualization, Y.L. and C.S.; methodology, C.S.; validation, Y.L. and C.S.; formal analysis, Y.L., C.S., X.C. and Q.F.; investigation, C.S.; resources, Y.H., C.W. and J.L.; data curation, C.S.; writing—original draft preparation, Y.L. and C.S.; writing—review and editing, Y.L., C.S., X.C. and P.C.; visualization, C.S.; supervision, C.S. and Q.F.; project administration, C.S. and Q.F.; funding acquisition, Q.F. All authors have read and agreed to the published version of the manuscript.

Funding: This research was funded by the National Natural Science Foundation of China (grant number 42075181, 42105097, 42275181), Science and Technology Planning Project of Guangzhou (grant number 2023A04J1544), Guangdong Major Project of Basic and Applied Basic Research (grant number 2020B0301030004), Guangdong Science and Technology Planning Project (grant number 2019B121201002), Key-Area Research and Development Program of Guangdong Province (grant number 2020B1111360003), and Guangdong Basic and Applied Basic Research Foundation (grant number 2023A1515010162).

Data Availability Statement: The data presented in this study are available on request from Chong Shen (shchong@mail3.sysu.edu.cn).

Acknowledgments: We give thanks for the support from the high-performance grid-computing platform of Sun Yat-sen University, and the Science and Technology Innovation Team Project of Guangzhou Meteorological Service (Urban Climate and Agrometeorology Innovation Team).

Conflicts of Interest: The authors declare no conflict of interest.

References

1. Hu, Z.; Yu, B. Review on methods calculating aerodynamic parameters over urban underlying surface. *J. Meteorol. Environ.* **2008**, *24*, 55–60.
2. Huang, J.; Zhong, Z.; Guo, W.; Lu, W. Statistical Features of Aerodynamic Effective Roughness Length Over Heterogeneous Terrain. *Acta Phys. Sin.* **2013**, *62*, 194–199. [[CrossRef](#)]

3. Liu, Y.; Guo, W.; Song, Y. Estimation of key surface parameters in semi-arid region and their impacts on improvement of surface fluxes simulation. *Sci. China Earth Sci.* **2015**, *45*, 1524–1536. [[CrossRef](#)]
4. Zhang, Q.; Yao, T.; Yue, P. Development and test of a multifactorial parameterization scheme of land surface aerodynamic roughness length for flat land surfaces with short vegetation. *Sci. China Earth Sci.* **2016**, *59*, 281–295. [[CrossRef](#)]
5. Hu, W.; Zhang, W.; Zhang, Y.; Guo, Z.; Liu, X. Variance Analysis on the Simulated and Observed Values of Underlying Surface Roughness in Gansu Corridor. *Plateau Meteorol.* **2010**, *29*, 51–55.
6. Wood, N.; Mason, P. The Pressure force induced by neutral, turbulent flow over hills. *Q. J. R. Meteorol. Soc.* **2010**, *119*, 1233–1267. [[CrossRef](#)]
7. Rotach, M.W. Determination of the zero plane displacement in an urban environment. *Bound. Layer Meteorol.* **1994**, *67*, 187–193. [[CrossRef](#)]
8. Martano, P. Estimation of Surface Roughness Length and Displacement Height from Single-Level Sonic Anemometer Data. *J. Appl. Meteorol.* **2000**, *39*, 708–715. [[CrossRef](#)]
9. Chen, J.; Wang, J.; Guang, T. An independent method to determine the surface roughness length. *Atmos. Sci.* **1993**, *17*, 21–26.
10. Lettau, H. Note on Aerodynamic Roughness-Parameter Estimation on the Basis of Roughness-Element Description. *J. Appl. Meteorol.* **1969**, *8*, 828–832. [[CrossRef](#)]
11. Lo, A.K. Determination of zero-plane displacement and roughness length of a forest canopy using profiles of limited height. *Bound. Layer Meteorol.* **1995**, *75*, 381–402.
12. Yang, R.; Friedl, M.A. Determination of Roughness Lengths for Heat and Momentum Over Boreal Forests. *Bound. Layer Meteorol.* **2003**, *107*, 581–603. [[CrossRef](#)]
13. Mikami, M.; Toya, T.; Yasuda, N. An analytical method for the determination of the roughness parameters over complex regions. *Bound. Layer Meteorol.* **1996**, *79*, 23–33. [[CrossRef](#)]
14. Patil, M.N. Aerodynamic drag coefficient and roughness length for three seasons over a tropical western Indian station. *Atmos. Res.* **2006**, *80*, 280–293. [[CrossRef](#)]
15. Zhou, Y.; Sun, X.; Zhu, Z.; Wen, X.; Tian, J.; Zhang, R. Comparative research on four typical surface roughness length calculation methods. *Geogr. Res.* **2007**, *26*, 887–896.
16. Zhang, Q.; Zeng, J.; Yao, T. Interaction of aerodynamic roughness length and windflow conditions and its parameterization over vegetation surface. *Chin. Sci. Bull.* **2012**, *57*, 647–655. [[CrossRef](#)]
17. Xing, L. The Aerodynamic Roughness Length of Chinese Surface Vegetation Based on MODIS and GLAS Data Inversion of Time-Serials. Master's Thesis, Capital Normal University, Beijing, China, 2012.
18. Liu, W.; Wei, X.; Shi, W.; Dong, W.; Zheng, Z.; Zhu, X.; Wei, Z. The Calculation of zero-plane displacement and aerodynamic roughness of heterogeneous terrain—With the evergreen broad-leaf forest in Zhuhai as an example. *J. Trop. Meteorol.* **2016**, *32*, 524–532.
19. Liu, Y.; Fang, X.; Luan, Q. Estimation of roughness length of Beijing area based on satellite data and GIS technique. *Plateau Meteorol.* **2016**, *35*, 1625–1638.
20. Mao, Y.; Liu, S.; Liu, J. Study of Aerodynamic Parameters on Different Underling Surfaces. *Acta Meteorol. Sin.* **2006**, *64*, 325–334.
21. Zhang, W.; Zhang, Y.; Lu, X.; Guo, Z.; Wang, X. Analysis on Heterogeneous Underlying Surface Roughness Length in Semi-Arid Mountains Area of Loess Plateau, China. *Plateau Meteorol.* **2009**, *28*, 763–768.
22. Ju, Y. Research on Dynamic Roughness and Thermodynamic Roughness of Different Underlying Surface Types. Master's Thesis, Nanjing University of Information Science and Technology, Nanjing, China, 2012.
23. Yao, T.; Zhang, Q.; Yin, H. The Annual Variation and Its Influencing Mechanism of Surface Roughness Length of Yuzhong in Semi-arid Areas. *J. Appl. Meteorol. Sci.* **2014**, *25*, 454–462.
24. Li, S.; Lv, S.; Liu, Y.; Zhang, Y.; Ao, Y.; Gao, Y.; Cheng, S.; Shang, L. Determination of Aerodynamical Parameter in Maqu Area in the Upper Reach of Yellow River and Its Application in Land Surface Process Model. *Plateau Meteorol.* **2010**, *29*, 1408–1413.
25. Sun, G.; Hu, Z.; Wang, J.; Xie, Z.; Lin, Y.; Huang, F. Upscaling analysis of aerodynamic roughness length based on In situ data at different spatial Scales and remote sensing in North Tibetan plateau. *Atmos. Res.* **2016**, *176–177*, 231–239. [[CrossRef](#)]
26. Lu, S.; Zuo, H.; Guo, Y.; Chen, J.; Feng, K.; Wang, S.; Wu, L. Modification and Simulation of Key Parameters in Land Surface Process in Desert Underlying Surface. *Arid Zone Res.* **2017**, *34*, 551–563.
27. Chen, S.; Lv, S. Calculation of Roughness Length of Desert and Its Application in Land Surface Process Model. *J. Desert Res.* **2013**, *33*, 174–178.
28. Zheng, D.; Velde, R.V.D.; Su, Z.; Booij, M.J.; Hoekstra, A.Y. Assessment of Roughness Length Schemes Implemented within the Noah Land Surface Model for High-Altitude Regions. *J. Hydrometeorol.* **2014**, *15*, 921–937. [[CrossRef](#)]
29. Huang, Y.; Salama, M.S.; Su, Z.; Velde, R.V.D.; Zheng, D.; Krol, M.S.; Hoekstra, A.Y.; Zhou, Y. Effects of Roughness Length Parameterizations on Regional Scale Land Surface Modelling of Alpine Grasslands in the Yangtze River Basin. *J. Hydrometeorol.* **2016**, *17*, 1069–1085. [[CrossRef](#)]
30. Shen, C.; Shen, A.; Tian, C.; Zhou, S.; Zhu, L.; Chan, P.; Fan, Q.; Fan, S.; Li, W. Evaluating the impacts of updated aerodynamic roughness length in the WRF/Chem model over Pearl River Delta. *Meteorol. Atmos. Phys.* **2020**, *132*, 427–440. [[CrossRef](#)]
31. Guangdong Statistical Yearbook on Agriculture Editorial Committee. *Guangdong Statistical Yearbook on Agriculture (2019)*; China Statistics Press: Beijing, China, 2019.
32. Raupach, M.R. Drag and drag partition on rough surfaces. *Bound. Layer Meteorol.* **1992**, *60*, 375–395. [[CrossRef](#)]

33. Raupach, M.R. Simplified expressions for vegetation roughness length and zero-plane displacement as functions of canopy height and area index. *Bound. Layer Meteorol.* **1994**, *71*, 211–216. [[CrossRef](#)]
34. Jasinski, M.F.; Borak, J.; Crago, R. Bulk surface momentum parameters for satellite-derived vegetation fields. *Agric. For. Meteorol.* **2005**, *133*, 55–68. [[CrossRef](#)]
35. Zeng, X.; Shaikh, M.; Dai, Y.; Dickinson, R.E.; Myneni, R. Coupling of the Common Land Model to the NCAR Community Climate Model. *J. Clim.* **2002**, *15*, 1832–1854. [[CrossRef](#)]
36. Liu, M.; Xing, Y.; Wu, H.; You, H. Study on Mean Forest Canopy Height Estimation Based on ICESat-GLAS Waveforms. *For. Res.* **2014**, *27*, 309–315.
37. Powers, J.G.; Klemp, J.B.; Skamarock, W.C.; Davis, C.A.; Dudhia, J.; Gill, D.O.; Coen, J.L.; Gochis, D.J.; Ahmadov, R.; Peckham, S.E. The weather research and forecasting model: Overview, system efforts, and future directions. *Bull. Am. Meteorol. Soc.* **2017**, *98*, 1717–1737. [[CrossRef](#)]
38. Chang, M.; Fan, S.; Wang, X. Impact of refined land-cover data on WRF performance over the Pearl River Delta region, China. *Acta Sci. Circumstantiae* **2014**, *34*, 1922–1933.
39. Shen, C.; Shen, A.; Cui, Y.; Chen, X.; Liu, Y.; Fan, Q.; Chan, P.; Tian, C.; Wang, C.; Lan, J.; et al. Spatializing the roughness length of heterogeneous urban underlying surfaces to improve the WRF simulation-part 1: A review of morphological methods and model evaluation. *Atmos. Environ.* **2022**, *270*, 118874. [[CrossRef](#)]
40. Liu, Y.; Wang, T. Worsening urban ozone pollution in China from 2013 to 2017—Part 1: The complex and varying roles of meteorology. *Atmos. Chem. Phys.* **2020**, *20*, 6305–6321. [[CrossRef](#)]
41. Hu, J.; Chen, J.; Ying, Q.; Zhang, H. One-year simulation of ozone and particulate matter in China using WRF/CMAQ modeling system. *Atmos. Chem. Phys.* **2016**, *16*, 10333–10350. [[CrossRef](#)]
42. Hong, Y.; Liu, Y.; Chen, X.; Fan, Q.; Chen, C.; Chen, X.; Wang, M. The role of anthropogenic chlorine emission in surface ozone formation during different seasons over eastern China. *Sci. Total Environ.* **2020**, *723*, 137697. [[CrossRef](#)]
43. Tuccella, P.; Curci, G.; Visconti, G.; Bessagnet, B.; Menut, L.; Park, R.J. Modeling of gas and aerosol with WRF/Chem over Europe: Evaluation and sensitivity study. *J. Geophys. Res. Atmos.* **2012**, *117*, D03303. [[CrossRef](#)]

Disclaimer/Publisher’s Note: The statements, opinions and data contained in all publications are solely those of the individual author(s) and contributor(s) and not of MDPI and/or the editor(s). MDPI and/or the editor(s) disclaim responsibility for any injury to people or property resulting from any ideas, methods, instructions or products referred to in the content.